Journal of Analytical and Applied Pyrolysis 95 (2012) 1–13

Contents lists available at SciVerse ScienceDirect

Journal of Analytical and Applied Pyrolysis

journal homepage: www.elsevier.com/locate/jaap

Review

Mathematical modeling of rubber tire pyrolysis

Augustine Quek, Rajasekhar Balasubramanian*

Department of Civil and Environmental Engineering, Faculty of Engineering, National University of Singapore, Block E1A #02-19, 9 Engineering Drive 1, Singapore 117576, Singapore

ARTICLE INFO

Article history:
Received 27 September 2011
Accepted 17 January 2012
Available online 25 January 2012

Keywords:
Tires
Activation
Pyrolysis
Waste
Resource recovery
Modeling

ABSTRACT

This article provides a critical review of past efforts over the last three decades at modeling the pyrolysis and gas activation of waste tires. The various forms of the Arrhenius kinetic rate equation as well as other forms of mathematical descriptions related to pyrolysis of waste tires are reviewed. In addition to reaction kinetics, other aspects of the tire pyrolysis such as heat and mass transfer, and reactor-specific models are also reviewed. Both one-step/component and multi-step/component pyrolysis models are discussed in the review. The multi-component models are based on the actual chemical components such as natural rubber and other additives. Kinetic constants reported in the literature are also analyzed.

Contents

1. Introduction

One of the major waste streams in the urban environment is waste tires. It was estimated that around 52.5 million equivalent passenger unit (EPU) tires reached their end of life in Australia (1 EPU = 8 kg). Approximately 64% of these tires went to landfill or were illegally dumped or stockpiled, while only 13% were recycled [1]. The European Community generated an estimated 1.5 million used tires in 1989 [2], which have swelled to 2.5 million tons within a decade [3]. In the United States alone, approximately 500 million scrap tires were generated in 2007, with about 128 million used tires already currently stockpiled throughout the country [4]. In 1998, world production and sales of tires were estimated to have attained a new milestone by passing over the 1 billion mark, with 2007 estimates reported at 1.3 billion tires [5]. Since it is generally accepted that for every tire sold in the market another joins the waste stream, approximately 1.3 billion tires reach the end of their life cycle annually. Rapid urbanization in many developing countries is expected to increase this solid waste further in future.

Waste tires are recalcitrant to natural degradation [6]. The vulcanized rubber consists of long chain polymers (polyisoprene, polybutadiene, and styrene–butadiene copolymers) that are cross-linked with sulfur bonds and are further protected by antioxidants and antiozonants that resist degradation [7]. In landfills, rubber tires tend to float to the top due to trapped gases, thus breaking landfill covers [6]. Combustion of tires produces toxic gases,

* Corresponding author. Tel.: +65 65165135; fax: +65 67744202.
E-mail address: ceerbala@nus.edu.sg (R. Balasubramanian).

0165-2370/$ – see front matter © 2012 Elsevier B.V. All rights reserved.
doi:10.1016/j.jaap.2012.01.012

which contain carcinogenic and mutagenic chemicals [7], so tire incineration requires expensive air emissions control systems.

Pyrolysis has been shown to be a technically feasible way to recover valuable products such as combustible gases, fuels and chemicals, activated carbon, etc., from waste tires [8]. Pyrolysis is a process in which organic materials are thermally decomposed into simpler constituent components when subjected to high heat, under an oxygen-free atmosphere [8]. However, pyrolysis of waste tires has still not been commercially viable despite several attempts at commercialization [9]. Therefore, the pyrolysis process of waste tires has been investigated in detail using numerous approaches by various researchers over the decades in an effort to understand its kinetics and mechanisms [2,3,8–63]. One popular approach to understand the pyrolysis process and provide mechanistic insights into it is to develop appropriate mathematical models. Various models have been used, including reaction rate kinetic models, heat and mass transfer models, etc. These models that describe the tire pyrolysis have been widely used among the research community to examine its technical viability of tire pyrolysis [8–63]. There is thus a need to synthesize, qualitatively and quantitatively, these past research efforts over the last few decades.

This review article critically examines mathematical models that describe the pyrolysis of tires as reported in the literature over the last three decades. The features of models used to describe the pyrolysis of waste tyres are discussed in terms of their respective strengths and weaknesses, or their self-sufficiency to provides technical insights into the pyrolysis process together with the existing modeling theories for the activation of tyre carbon chars. Reactor-specific models which describe the tire pyrolysis process for only a particular type of reactor are also discussed.

2. Material and methods

2.1. Tire composition

Tire pyrolysis is strongly dependent on tire composition and the type of inter- and intra-molecular bonding that exists among the polymers that makes up the tires [7]. Tire composition thus influences tire thermal decomposition mechanisms under various conditions, which in turn affects the type of mathematical models that can be used to describe the pyrolysis process.

Although the details of the formula for each brand of tire have been a closely guarded secret, the main components of a rubber tire are well known. There are three known polymers that are used for the rubber components, namely polyisoprene (natural rubber), polybutadiene and polystyrene–butadiene. The monomers are shown in Table 1.

In addition, other chemicals and materials added during the tire manufacturing process include vulcanization accelerators and retarders, fillers, softeners and extenders, plasticizers, activators and protectants [7]. Three examples of tire constituents as reported in the literature, spanning three decades, from the 1980s to the 2000s, are shown in Table 2.

2.2. Methodology

A common thermal method of material analysis is the use of a thermogravimetric analyzer (TGA). The TGA is basically a thermobalance, which is able to record the weight of the material which is being heated to high temperatures. Despite the apparent simplicity of the TGA, different polymers such as those found in tires can be distinguished and identified using the TGA method [12–16].

An attempt at correlating major compounds in tires with the thermogravimetric results was made by Williams and Besler [12]. They heated three different tires at different heating rates, and compared the results with thermograms of three rubber compounds (NR, BR, and SBR). They found that areas of major weight loss on the thermograms correspond to the weight loss patterns of one or more of the three rubbers, and were able to derive kinetic parameters using the Arrhenius equation and its derived equations (Equations (1)–(7)).

Table 1
Rubber monomers in tires [7].

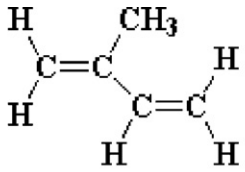

isoprene

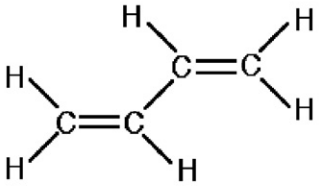

butadiene

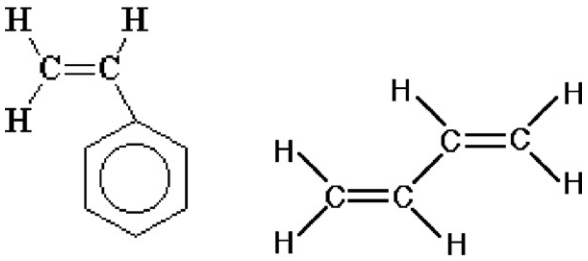

styrene-butadiene (1 styrene, 3 butadiene)

A similar attempt was made later by Seidelt et al. [13]. They showed that tires are made up of three main components, natural rubber (polyisoprene), styrene–butadiene rubber copolymer (SBR) and additives (sulfur, zinc oxide (ZnO), carbon black). Through a trial-and-error process, the derivative thermogravimetry (DTG) curves of these components in the right ratios can be superimposed on DTG curves of actual tires. Using kinetic parameters obtained for each component, Seidelt et al. [13] performed a similarity merging to show a good agreement with experimental results.

It is now generally accepted that different zones can be distinguished in the thermogram due to devolatilization of its compounds [8,12–16]. These different tire compounds thermally decompose independently of each other, with little interaction. The non-dependency of polymer thermal decomposition is the basis for the construction of most tire pyrolysis models.

3. Results and discussion

3.1. General features

Modeling of tire pyrolysis relies almost exclusively on data from TGA and DTG, where model equations are used to deconvolute the peaks in the thermograms [8]. Typically, these thermograms would contain the rate of mass loss with respect to either time or temperature.

Table 2
Tire constituents as reported in the literature.

Source	Aguado et al. [10]		CIWMB [7]		Bouvier et al. [11]	
Compound name and mass %	Natural rubber (SMR 5CV), styrene–butadiene rubber (SBR 1507)	29.59%	Styrene butadiene	46.78%	SBR	43.5%
		29.59%				
	Carbon black (ISAF N220), stearic acid	29.59%	Carbon black	45.59%	Carbon black	32.6%
		0.59%	Aromatic oil	1.74%	Extender oil	21.7%
	Zinc oxide	2.96%	Zinc oxide	1.40%	ZnO and sulfur	2.2%
	Phenolic resin	2.37%	Stearic acid	0.94%		
	Aromatic oil	2.37%	Antioxidant 6C	1.40%		
	IPPD (*N*-isopropyl-*N*′-phenyl-*p*-phenylendiamine)	0.89%				
	Sulfur	0.89%	Sulfur	1.17%		
	CBS (*n*-cyclohexyl-2-benzothiazol-sulfenamide), H-7 (hexamethylentetramine)	0.89%	Accelerator CZ	0.75%		
		0.18%				
	PVI (*n*-cyclohexylthio-phthalimide)	0.12%	Wax	0.23%		

Most pyrolysis models assume a kinetic rate-limiting type of reaction and do not consider heat or mass transfer limitations in a reactor [8]. Therefore, most reactions are of the form:

$$r = kC^n \tag{1}$$

where r, the rate of reaction is proportional to the nth order of the mass concentration of the reactant C, k is the rate constant. A common method in modeling pyrolytic reactions is to utilize Arrhenius type equations, where the rate constant is of the form:

$$k = Ae^{-\frac{E_a}{RT}} \tag{2}$$

where k is the reaction rate constant (min^{-1}), A is the pre-exponential factor (min^{-1}), E_a the activation energy of reaction (J/mol), R is the gas constant ($8.314\,\mathrm{J\,mol^{-1}\,K^{-1}}$) and T the temperature of reaction. This gives the classic pyrolysis model as a function of both temperature and reactant mass concentration:

$$r = Ae^{-\frac{E_a}{RT}}C^n \tag{3}$$

In this case, C may be substituted with the normalized mass fraction of the tire sample that has decomposed, X, as measured in the TGA.

$$X = \frac{m_o - m}{m_o - m_\infty}, \tag{4}$$

where m_o, m_∞ and m are the initial mass of the tire sample, the final mass after complete pyrolysis and the mass at any time during the pyrolysis.

Therefore, the rate of reaction, r, would be rate of mass loss of the tire sample. For isothermal conditions, the rate of mass loss with respect to time can be written as:

$$\frac{dX}{dt} = Ae^{-E_a/RT}(1-X)^n \tag{5}$$

For non-isothermal pyrolysis conditions where the heating rate is constant, i.e. $dT/dt = \beta$ [16], such that

$$\frac{dX}{dT} = \frac{1}{\beta}Ae^{-E_a/RT}(1-X)^n, \tag{6}$$

a linearized form of the differential equations (5) and (6) can be used [10,17] if certain assumptions are made. Equation (5) can be linearized to give the expression:

$$\ln\left(\frac{dX}{dt}\right) = \ln A - \frac{E_a}{RT} + \ln(1-X)^n. \tag{7}$$

If a first-order reaction is assumed ($n = 1$), and the values of $\ln[(\frac{dX}{dt})/(1-X)]$ are plotted against $-\frac{1}{T}$, the values of E_a and A can be obtained from the gradient and y-intercept, respectively. Similarly, equation (6) can be re-written as:

$$\ln\left(\frac{dX}{dT}\right) = \ln\frac{A}{\beta} - \frac{E_a}{RT} + n\ln(1-X) \tag{8}$$

with similar application to equation (7).

However, if an integral approach is used; integrating equation (6) yields the following equations:

for $n = 1$

$$\ln(1-X) = \frac{A}{\beta}\int e^{-E_a/RT}dT \tag{9}$$

for $n \neq 1$ (10)

$$\frac{(1-X)^{1-n}}{n-1} = \frac{A}{\beta}\int e^{-E_a/RT}dT. \tag{10}$$

There is no exact analytical solution to the integrals in equations (9) and (10), so approximations in the form of series expansions are often used. The most commonly used approximation expansion is the one developed by Coats and Redfern [64]. They used the substitution

$$\int_x^\infty e^{-t}t^{-\alpha}dt \approx x^{1-\alpha}e^{-x}\sum_{n=0}^{\infty}\frac{(-1)^n(\alpha)_n}{x^{n+1}} \quad \text{for} \quad x \to \infty \tag{11}$$

which provides the expansion of the first two terms:

$$\frac{A}{\beta}\int e^{-E_a/RT}dT = \frac{A}{\beta}\frac{RT^2}{E_a}\left[1 - \frac{2RT}{E_a}\right]e^{-E_a/RT}. \tag{12}$$

Equation (12) can be equated to the logarithmic form in equations (9) or (10), depending on the order of reaction. In both cases, regardless of whether the differential or integral form is used, a best fit curve is normally used to estimate the pyrolysis parameters of activation energy (E_a) and pre-exponential factor (A) from the data of m versus temperature (T) or time (t) [14–19]. Therefore, the main difference in the various tire pyrolysis models is the approximation method in obtaining E_a and A.

Another important point to note when using models with the Coats and Redfern approximation is that it cannot be used to distinguish between different mechanisms [65]. The Coats and Redfern approximation was also found to be unable to give accurate kinetic parameters when more than one reaction mechanism is occurring [65].

For the models presented above that are used to describe tire pyrolysis, three main assumptions are required:

a. Major components in the tire (processing oils, polyisoprene, polybutadiene, styrene–butadiene copolymer) thermally decompose independently of each other without any interaction among them.
b. Each of these decomposition reactions follow only one mechanism and is irreversible.
c. Only data from the DTG curve are needed in order to estimate the initial tire composition (component identification and component mass), the rate of devolatilization of each component, and its kinetic parameters.

3.2. Single-stage reaction rate models

There are two different approaches used in applying the models. The more popular approach is to model each major component of the tire separately [13–15,18–21]. Each component would be represented by a peak in the TGA curve, to which the Arrhenius type equation can be fitted. The other method is to assume a single peak and applying only one set of kinetic parameters [10,22–25]. However, several arguments can be made against the second approach, the 'single parameter set' method. Firstly, the Coats–Redfern approximation cannot be used to accurately obtain kinetic parameters when multiple reactions, with different mechanisms, occur simultaneously [65].

Zabaniotou et al. [23] used equation (9) in modeling flash pyrolysis of used tire particles in a helium atmosphere as one reaction, but obtained a value for the activation energy that is much lower than others reported in the literature. Aguado et al. [10] linearized the kinetic expression that incorporates the Arrhenius type equation (equation (8) with $n = 1$). They showed that the same values obtained at higher temperatures fit the same line for all heating rates, while the results are more diffuse at lower temperatures. By using only the range of temperatures that fit the data, an apparent activation energy and frequency factor can be calculated [10].

However, a closer look at the data reveals that while the data plots for heating rates of 2 K/min and 10 K/min follow each other very closely, the data points for 5 K/min do not fall in between these two rates. This implied that a more complicated series of reactions are occurring than the authors contend [10]. They then used a microreactor and measured different products evolved for tires pyrolyzed under a helium atmosphere. Different kinetic parameters were calculated for 13 of the products measured [10], proving that tire pyrolysis is not a singular reaction.

This was also the case for Unapumnuk et al. [25], which performed nonlinear regression on the data sets to obtain a single overall E_a, A and n (order of reaction) for each heating rate. Though claims were made for good agreement between their results and others, the mean values obtained were significantly different from those from previous studies, with high standard deviations. However, Unapumnuk et al. [25] also acknowledged that the ingredients of tires are complicated and contain additive and cross-linking agents. The kinetics of tire decomposition is initially rate controlled, but later becomes more diffusion controlled [25].

Sachin and Giridhar [26] used the same linearized equation (equation (8)) to calculate the activation energies for the pyrolysis of *cis*-1,4 polybutadiene with a cobalt Fischer–Tropsch catalyst and without a catalyst under high temperature conditions. However, they found no difference in the pyrolysis rates between the two conditions. Therefore, the rate of reaction cannot be simply described by assuming a single reaction, with only one set of constants or values. Instead, kinetic constants for pyrolysis reactions of the three main compounds must be described separately. For this approach, a consensus seems to appear in the literature on tire pyrolysis DTG data as having a 'two-peak, three-steps' kinetic analysis modeling. This corresponds to the evolution of major components of a tire, such as extender oil, natural rubber (NR) and manufactured rubber (SBR, BR) [18]. This was the approach of Aylón et al. [21] and Seidelt et al. [13] who attempted to use kinetic constants for each of the tire components to fit experimental data. While the fit by them was reasonably good, overlapping regions for NR and SBR did not show a good fit. This was also the case when DTG data of each component were used to fit into DTG data for tire pyrolysis [13,21]. A good fit at the two ends was achieved, except in the overlapping region in mid-process. The composition for the best fit for tire sidewall (37%IR/63% SBR – 37.5% oil, styrene 23.5%) was different from tire tread (13%IR/87%SBR – 37.5% oil, 40% styrene) [13]. Another model approach is to use the sum of errors using nonlinear least squares regression, by calculating a fraction of contribution for each component to the global reaction (11.6% additives,.32.6% IR, 18%SBR, 37.8% carbon black) [21]. Using this method, Aylón et al. [21] successfully validated their model results with a fixed bed reactor.

Senneca et al. [14] applied the Arrhenius model equations to tire pyrolysis at heating rates from 5 to 900 K/min. They noted that the Arrhenius plots did not overlap with each other and therefore, tire pyrolysis could not be represented as a single reaction. Senneca et al. [14] further observed that the two peaks merged into one at higher heating rates and attributed this merging to the decreasing extent of cyclization/cross-linking as the heating rate was raised. They further postulated that cyclization limits the extent of pyrolysis, with the observed second peak being the result of the cyclized residue degradation. Their observations of higher primary-to-secondary pyrolysis product ratios at higher heating rates also support the assertion that the apparent activation energy of the cyclization reaction is smaller than the activation energy of pyrolysis reaction in the first peak (primary pyrolysis). An equation to model the cyclization reaction was proposed by Senneca et al. [14] by expressing the primary pyrolysis yield, η_{pv}, as:

$$\eta_{pv} = \frac{k_1}{H_r}\int_{T_{min}}^{T_{max}} \exp\left\{-\frac{E_{a1}}{RT} - \frac{RT^2}{H_r}\left[\frac{k_1}{E_1}\exp\left(-\frac{E_{a1}}{RT}\right) + \frac{k_2}{E_2}\exp\left(-\frac{E_{a2}}{RT}\right)\right]\right\} dT, \quad (13)$$

where T_{min} and T_{max} are the initial and final temperatures of the pyrolysis run, k_1 and k_2 are the primary and secondary (cyclization) pyrolysis rate constants respectively, and E_{a1} and E_{a2} are the activation energies of the primary and secondary (cyclization) pyrolysis, respectively.

The extensive use of logarithm involving the Arrhenius rate equation in these methods might conceal errors or other irregularities in the data. Other problems with these methods have also been highlighted by Conesa et al. [27]. They pointed out that taking the logarithm of logarithm present a similar problem of concealing data. Conesa et al. [27] also pointed out that the Arrhenius reaction rate methods apply only to one reaction. For more than one reaction occurring simultaneously, such as tire pyrolysis, a deconvolution must be done. Lastly, there is the problem of using the programmed temperature in the TGA, instead of the tire particle temperature.

3.3. Heat and mass transfer

To overcome the temperature limitation in pyrolysis models, heat and mass transfer have to be incorporated into a kinetics model to describe the actual temperature of the tire during pyrolysis. Heat and mass transfer processes are important because tire decomposition during pyrolysis is initially rate controlled due to predominance of surface reactions, but becomes more diffusion controlled in the final stages [25]. An early attempt to overcome the heat transfer problem is the transient 'bubble' model of a single tire particle developed by Yang and co-workers [62]. The model

attempts to predict the temperature gradient through the particle and the subsequent volatile loss, but is not easily scalable to large masses of particles.

Yang and Roy [29] later used a different form of thermogravimetry, differential thermal analysis (DTA) to quantitatively measure the enthalpy change during the pyrolysis of tire rubbers. This method heats both the sample and a reference material and records the temperature differences. According to Yang and Roy's [29] model the "mass-difference baseline method" uses the DTA curves for a small sample as the baseline for a larger mass sample. The method was tested for pyrolysis temperatures up to 600 °C, and could determine the heat capacity changes as well as the heat of reaction and heat of evaporation, which occurred during the enthalpy changes of the tire rubbers subjected to decomposition. However, the authors concluded that accuracy of this method is still not high enough for high accurate enthalpy measurement.

Larsen et al. [30] constructed a detailed model of tire pyrolysis that included internal and external heat transfer, three parallel reactions and reaction enthalpy effects. They assumed first order reaction using the Arrhenius equations for the parallel reactions, while assuming heat transfer in the radial direction in a cylinder. However, the calculated results for the derivative TGA showed two peaks, while the experimental results showed only one. This could be due to their selection of parameters, which might not have captured the pyrolysis process accurately enough. Larsen et al. [30] also conducted a sensitivity analysis on their model where the various parameters were varied by ±25%, and the pyrolysis time was calculated. The pyrolysis time was found to be most sensitive to changes in activation energies of the reactions of the tire's constituent compounds, with a change of more than 96% change in the pyrolysis time. This showed that the chemical kinetics is more important than heat transfer in predicting the tire pyrolysis times.

The model developed by Quek and Balasubramanian [31] takes into account both reaction rates and mass transfer limitations. It was also tested on thermal degradation of at least two different tires, at three different heating rates. In addition to the Arrhenius reaction equation, they used a simplified form of Newton's heat transfer and the third order Avrami-Erofe'ev equation for intra-particle mass transfer:

$$T(t) = T_f + (T(0) - T_f)e^{-\gamma t} \tag{14}$$

$$w_i = w_{i,o}4(X_i)[-\ln(X_i)]^{3/4} \tag{15}$$

where $T(t)$ is the temperature at time t for each data point, T_f is the furnace temperature, external to the rubber sample, and γ is the time constant characteristic of the system. The model showed that frequency factors increased and time constants decreased with increasing heating rates. The model also showed the change in the behavior of individual tire components when the heating rates were increased above 30 K/min. The result obtained by Quek and Balasubramanian [31] indicated that the heating rates rather than the absolute temperature can significantly affect pyrolysis reactions.

3.4. Multiple component models

Teng et al. [32] assumed a first order reaction and applied the kinetic equations only at their maximum points i.e. when $d^2m/dT^2 = 0$. At the point of inflexions, they derived a linear equation from the derivative of equation (6)

$$\ln(\beta T^2) = \ln\left(\frac{AR}{E_a}\right) - \frac{E_a}{RT}. \tag{16}$$

By plotting $\ln(\beta T^2)$ against $(1/T)$, the values of E_a and A can be obtained, for each peak temperature at which the turning point occurs. Using this approach, Teng et al. [32] determined the kinetic parameters (E_a and A) for each component by assuming the tire to be composed of three components. The values of these constants are shown in Table 3.

The researchers also approximated $E_a/RT \gg 1$, and expressed the mass of volatiles evolved using only the first term of equation (12), obtaining:

$$(1 - V_m) = \exp\left[-\frac{A}{\beta}\frac{RT^2}{E_a}(e^{-E_a/RT})\right], \tag{17}$$

where V_m is the mass fraction of volatiles evolved. They plotted this equation using the values obtained from equation (13) and compared with their experimental data, which showed a good visual fit.

This is similar to the Kissinger method [66], which can be employed to calculate the activation energies. Based on the change in the position of the peak maxima T_{max} under different heating rates β, a linear regression of $\ln \beta/T_{max}^2$ vs. $1/T_{max}$ plot gives the activation energy of the thermal degradation reaction.

Another approach by Leung and Wang [18] was to model tire pyrolysis kinetics as two separate regions: a high temperature region and a lower temperature region. Their proposed model assumed two reactions in the tire rubber pyrolysis, corresponding to the degradation of the main components of tires. The pyrolysis rate was assumed to be the sum of two reaction rates, such that:

$$\frac{dM}{dt} = \frac{dm_1}{dt} + \frac{dm_2}{dt}, \tag{18}$$

where M is the total mass of the tire sample, m_1 and m_2 are masses of the undergoing reactions in the lower and higher temperature regions, respectively. By using equations (6) and (7) in equation (18), and normalizing the mass loss rates, for tire rubber pyrolysis at different heating rates, Leung and Wang [18] obtained the kinetic parameters for the two different temperature regions. Using these obtained parameters; they recalculated the normalized mass loss rates using equations (9) and (12) and plotted this theoretical line against the experimental data.

Using the same set of equations in a later work, Leung and Wang [19] derived another two different approaches to model tire pyrolysis. The three-component simulation model assumes that tires comprise only three major degradable components, with oil, moisture, plasticizer and additives lumped as one component, while NR, BR. SBR and their combination are the next two components.

$$\frac{dM}{dt} = \sum_{i=1}^{3}\frac{dm_i}{dt} \tag{19}$$

and from equation (5), with $n = 1$:

$$\ln\sum_{i=1}^{3}\frac{dX_i}{dt} = \ln\left[Ae^{-E_a/RT}(1 - X_i)\right], \tag{20}$$

where M the total mass of the sample, m_i the mass of the ith component, and X_i the normalized mass fraction.

The three-elastomer simulation model assumes that all mass volatilization are due only to the elastomers NR, BR and SBR and their respective oil components. Therefore, the model effectively incorporates six components in the following equation:

$$\frac{dX_T}{dt} = \sum_{i=1}^{6}\frac{dX_i}{dt} = \sum_{i=1}^{6}A_i\exp\left(-\frac{E_{a,i}}{RT_i}\right)(M - m_{\infty i})^{n_i - 1}\left(X_{i,\infty} - X_i\right)^{n_i}, \tag{21}$$

where n_i is either equal to 1 or 2 for each component. M is the total mass of the initial tire sample, $m_{\infty i}$ is the final mass of component i.

Table 3
Model constants from literature.

Reference	Condition	E_a (kJ/mol)	A (min^{-1})
Piatkowski and Steinfeld [46]		C_1 = 132.4	$C_1 = 2.46 \times 10^{10}$
		C_2 = 168.9	$C_2 = 1.21 \times 10^{12}$
		C_3 = 155.6	$C_3 = 9 \times 10^4$
Mui et al. [61]	β = 1, 5, 10, 20 K/min	Component 1 = 42.8, 51.3, 50.3, 40.5	Component 1 = 27, 426, 501, 114
		Component 2 = 127, 116.3, 102.8, 77.2	Component 2 = 1.13×10^9, 1.45×10^8, 1.9×10^7, 2.98×10^5
		Component 3 = 152.2, 158, 237.1, 171.4	Component 3 = 5.26×10^{16}, 1.21×10^{11}, 1.13×10^{17}, 3.16×10^{12}
Lopez et al. [38]	1 atm	Step 1 = 50.6 ± 4.9	Step 1 = 2.46 (±0.21) × 10^1
		Step 2 = 130.8 ± 4.9	Step 2 = 5. 63 (±0.53) × 10^7
	0.25 atm	Step 3 = 245.9 ± 18.9	Step 3 = 8.10 (±0.71) × 10^1
			Step 1 = 7.62 (±0.61) × 10^1
		Step 1 = 43.5 ± 3.9	Step 2 = 6.0 (±0.45) × 10^5
		Step 2 = 104.7 ± 9.2	Step 3 = 9.09 (±0.77) × 10^1
		Step 3 = 243.0 ± 20.9	
Mazloom et al. [55]	Thermal pyrolysis	$k_1 = 5.9 \times 10^3$	$k_1 = 2.01 \times 10^{-2}$
		$k_2 = 2.00 \times 10^3$	$k_2 = 1.42 \times 10^{-2}$
	Catalytic pyrolysis	k_3 = 0.00	$k_3 = 2.93 \times 10^{-3}$
		$k_4 = 2.91 \times 10^3$	$k_4 = 5.13 \times 10^{-3}$
		$k_1 = 5.59 \times 10^5$	k_1 = 0.51
		$k_2 = 6.48 \times 10^3$	k_2 = 1.06
		$k_3 = 3.48 \times 10^3$	k_3 = 1.94
		$k_4 = 1.24 \times 10^4$	k_4 = 5.13
		$k_5 = 4.64 \times 10^3$	k_5 = 1.28
Quek and Balasubramaniam [31]	β = 10–50 K/min	Oil = 43	Oil = 7.68×10^2–8.94×10^3
		NR = 207	NR = 1.74×10^{16}–1.18×10^{15}
		SBR = 152	SBR = 6.0×10^8–1.96×10^{11}
		BR = 215	BR = 2.68×10^{11}–3.41×10^{15}
Islam et al. [37]	β = 10 K/min (Low/Medium/High temperature region)	Bicycle/rickshaw = 65.42/118.35/108.85	Bicycle/rickshaw = $2.55 \times 105/6.4 \times 10^7/7.48 \times 10^7$
		Motorcycle = 74.94/130.25/110.8	Motorcycle = $8.57 \times 10^5/2.59 \times 10^7/8.66 \times 10^7$
		Truck = 74.42/115.8797.89	Truck = $4.1 \times 10^6/1.08 \times 10^8/3.25 \times 10^9$
	β = 60 K/min (Low/Medium/High temperature region)	Bicycle/rickshaw = 70.45/138.95/105.65	Bicycle/rickshaw = $5.8 \times 10^6/2.52 \times 10^8/5.79 \times 10^8$
		Motorcycle = 79.93/153.45/99.79	Motorcycle = $7.0 \times 10^6/1.68 \times 10^9/5.39 \times 10^8$
		Truck = 78.19/135.49/95.45	Truck = $6.4 \times 10^7/1.0510^9/6.72 \times 10^9$
Suuberg and Aarna [50]		138–150	2.73 (±0.7) × 10^5(×35–135)
Mui et al. [35]	β = 1, 5,10, 20 K/min Data presented here only for 5K/min	Three-component model	Three-component model
		Component 1 = 67.4 (Coats–Redfern)	Component 1 = 2.88×10^5(Coats–Redfern)
		Component 1 = 50.3 (Runge–Kutta)	Component 1 = 5.02×10^4 (Runge–Kutta)
		Component 2 = 180.0 (Coats–Redfern)	Component 2 = 2.02×10^{14} (Coats–Redfern)
		Component2 = 133.6 (Runge–Kutta)	Component 2 = 1.41×10^{12} (Runge–Kutta)
		Component3 = 111.0 (Coats–Redfern)	Component 3 = 3.98×10^7 (Coats–Redfern)
		Component 3 = 85.7 (Runge–Kutta)	Component 3 = 3.97×10^6 (Runge–Kutta)
		Four-component model	Four-component model
		Component 1 = 83.9 (Coats–Redfern)	Component 1 = 1.27×10^7 (Coats–Redfern)
		Component 1 = 52.1 (Runge–Kutta)	Component 1 = 7.31×10^4 (Runge–Kutta)
		Component 2a = 170.6 (Coats–Redfern)	Component 2a = 2.21×10^{13} (Coats–Redfern)
		Component 2a = 132.7 (Runge–Kutta)	Component 2a = 1.29×10^{12} (Runge–Kutta)
		Component 2b = 175.1 (Coats–Redfern)	Component 2b = 1.29×10^{14}(Coats–Redfern)
		Component 2b = 155.3 (Runge–Kutta)	Component 2b = 6.82×10^{13} (Runge–Kutta)
		Component 3 = 136.1 (Coats–Redfern)	Component 3 = 3.17×10^9 (Coats–Redfern)
		Component 3 = 106.6 (Runge–Kutta)	Component 3 = 2.54×10^8 (Runge–Kutta)
		Five-component model	Five-component model
		Component 1 = 78.0 (Coats–Redfern)	Component 1 = 3.41×10^6 (Coats–Redfern)
		Component 1 = 50.2 (Runge–Kutta)	Component 1= 6.22×10^4 (Runge–Kutta)
		Component 2a = 196.6 (Coats–Redfern)	Component 2a = 5.69×10^{15} (Coats–Redfern)
		Component 2a = 140.4 (Runge–Kutta)	Component 2a = 5.49×10^{12}(Runge–Kutta)
		Component 2b = 178.2 (Coats–Redfern)	Component 2b= 5.71×10^{12} (Coats–Redfern)
		Component 2b = 119.1 (Runge–Kutta)	Component 2b = 5.12×10^{10} (Runge–Kutta)
		Component 3a = 144.3 (Coats–Redfern)	Component 3a = 1.21×10^{11} (Coats–Redfern)
		Component 3a = 140.3 (Runge–Kutta)	Component 3a = 1.58×10^{11}(Runge–Kutta)
		Component 3b = 140.7 (Coats–Redfern)	Component 3b = 6.50×10^9(Coats–Redfern)
		Component 3b = 81.2 (Runge–Kutta)	Component 3b = 3.40×10^6 (Runge–Kutta)

Table 3 (*Continued*)

Reference	Condition	E_a (kJ/mol)	A (min^{-1})
Olazar et al. [52]		Tire to intermediate = 46.1 Tire to gas = 63.1 Tire to liquid = 40.1 Tire to aromatics = 89.3 Intermediate to aromatics = 36.3 Intermediate to tar = 14.1 Intermediate to char = 20.5	Tire to intermediate = 6.82×10 Tire to gas = 3.52×10^{-7} Tire to liquid=1.30×10 Tire to aromatics = 5.35×10^{3} Intermediate to aromatics = 5.00×10^{-1} Intermediate to tar = 2.36×10^{-3} Intermediate to char = 4.79×10^{-1}
Larsen et al. [45]	Tire char combustion	193 ± 28	$1.5 \pm 5.1 \times 10^{10}$
Aranda et al. [41]	Steam pyrolysis $n = 0.6$	175.9	2.22×10^{-2}
Galvagno et al. [33]	Component 1, $n = 0.84$ Component 2, $n = 0.98$ Component 3, $n = 0.95$ $\beta = 10$–50 K/min	Component 1 = 58.7 Component 2 = 156.6 Component 3 = 116.3	Component 1 = 8.9×10^{4} Component 2 = 7.4×10^{11} Component 3 = 8.2×10^{7}
Larsen et al. [30]	$\beta = 10$ K/min	Oil = 49.1 NR = 207 BR = 212	Oil = 6.0×10^{3} NR = 3.93×10^{14} BR = 1.05×10^{13}
Seidelt et al. [13]	NR = 2.0 SBR (23.5%PS/76.5%BR) = 0.7 BR first step = 0.9 BR second step = 0.8	NR = 254 SBR (23.5%PS/76.5%BR) = 143 BR first step = 194 BR second step = 202	NR = 7.23×10^{8} SBR (23.5%PS/76.5%BR) = 1.63×10^{4} BR first step = 9.82×10^{6} BR second step = 1.09×10^{6}
Aguado et al. [10]		98.6	7.35×10^{4}
Aylón et al. [21]		Additives = 70 Polymer 1 = 212 Polymer 2 = 265	Additives = 1.0×10^{4} Polymer 1 = 8.20×10^{14} Polymer 2 = 3.20×10^{17}
Olazar et al. [24]	Particle diameter = 0.8–4.0 mm Particle diameter = 0.1–0.8 mm	41.3 121.3	2.135 1.0×10^{6}
Sachin and Giridhar [26]		First stage = 34 Second stage = 208	NR
Murillo et al. [39,40]	$\beta = 8$ K/min	Volume model = 191.79 Modified-volume model = 191.4 Changing grain size model = 197.45 Random pore model = 197.7	Volume model = 6.43×10^{3} Modified-volume model = 9.16×10^{3} Changing grain size model = 1.13×10 Random pore model = 1.53×10
Zabaniotou et al. [23]	$\beta = 70$–90 K/s	65.6	5.10
Chen et al. [22]	$n = 1.98$ (Car) $n = 1.63$ (Truck)	Car = 147.6 Truck 148.1	Car = 7.57×10^{10} Truck = 5.02×10^{10}
Senneca et al. [14]	$\beta = 5$, 20, 100, 900 K/min	$R_1 = 168.7$ $R_2 = 83.14$ $R_3 = 169.6$	$R_1 = 1.00 \times 10^{13}$ $R_2 = 5.00 \times 10^{5}$ $R_3 = 1.00 \times 10^{12}$
Leung and Wang [19]	$\beta = 10$ K/min Three-component simulation model Three elastomer simulation model	Component 1 = 52.5 Component 2 = 164.5 Component 3 = 136.1 Oil = 43 NR = 207 Oil = 43 BR = 215 Oil = 48 SBR = 152	Component 1 = 2.0×10^{4} Component 2 = 6.3×10^{13} Component 3 = 2.3×10^{9} Oil = 4.5×10^{3} NR = $3.0 \times$ Oil = 2.3×10^{3} BR = 7.1×10^{14} Oil = 6.9×10^{3} SBR = 3.1×10^{10}
Conesa et al. [20]		$F1 = 83.6$ $F2 = 245.6$ $F3 = 201.7$ $F4 = 223.2$	$F1 = 2.84 \times 10^{6}$ $F2 = 4.64 \times 10^{14}$ $F3 = 4.15 \times 10^{14}$ $F4 = 3.79 \times 10^{8}$
Leung and Wang [18]	$\beta = 10$–60 K/min	Tire powder Low temperature range = 164.5–218.7 High temperature range = 99.1–136.1 Tire fiber Low temperature range = 152.0–210.1 High temperature range = NR	Tire powder Low temperature range = 6.3×10^{13}–1.1×10^{17} High temperature range = 1.0×10^{7}–2.3×10^{9} Tire fiber Low temperature range = 4.8×10^{11}–5.1×10^{17} High temperature range = NR

Table 3 (*Continued*)

Reference	Condition	E_a (kJ/mol)	A (min^{-1})
Sharma et al. [51]		k_{tr} = 24.4 ± 6.9 k_t = 35.7 ± 7.2 k_c = 158.4 ± 122.4 k_a = 0 k_{ac} = 0 k_s = 83.8 ± 27.4 k_{sc} = 0	k_{tr} = 4.0 ± 1.1 (h^{-1}) k_t = 1.0 ± 0.4 k_c = 1.2 ± 0.8 k_a = 6.8 ± 1.8 k_{ac} = 0 k_s = 3.6 ± 0.6 k_{sc} = 0
Conesa et al. [44]	β = 1,5, 25 K/min	$F1$ = 70 $F2$ = 212.6 $F3$ = 249.3	$F1 = 3.68 \times 10^5$ $F2 = 4.13 \times 10^{16}$ $F3 = 5.96 \times 10^{17}$
Lin et al. [17]	Styrene–butadiene rubber β = 3, 5, 10 K/min n = 2.09, 1.28, 1.90	Reaction 1 = 52.5 Reaction 2 = 150.6 Reaction 3 = 169.4	Reaction 1 = 2.3×10^3 Reaction 2 = 1.5×10^{10} Reaction 3 = 3.5×10^{10}
Lin et al. [34]	Polybutadiene rubber n = 1.27, 1.49	Reaction1 = 59.8 Reaction 2 = 197.0	Reaction1 = 2.8×10^3 Reaction 2 = 1.9×10^{13}
Conesa and Marcilla [43]		Calprene 416 = 232.2 (E_1), 289.0 (E_2) Calprene 484 = 72.9 (E_1), 462.5 (E_2) Calprene 248 = 45.1 (E_1), 211.8 (E_2), 290.1 (E_3) Calprene 1204 = 39.0 (E_1), 208.8 (E_2), 270.3 (E_3) Europrene Sol T 171 = 82.4 (E_1), 295.8 (E_2) Europrene Sol T 6302 = 266.8 (E_1), 384.5 (E_2) Polyisoprene = 68.4 (E1), 219.7 (E2), 225.7 (E3)	Calprene 416 = 7.69×10^{15} (E_1) = 4.31×10^{18} (E_2) Calprene 484 = 2.793×10^4 (E_1) = 1.821×10^{31} (E_2) Calprene 248 = 4.23×10 (E_1) = 2.98×10^{14} (E_2) = 5.64×10^{18} (E_3) Calprene 1204 = 9.758 (E_1) = 4.03×10^{13} (E_2) = 2.20×10^{17} (E_3) Europrene Sol T 171 = 1.01×10^6 (E_1) = 1.99×10^{19} (E_2) Europrene Sol T 6302 = 2.47×10^{18} (E_1) = 3.18×10^{25} (E_2) Polyisoprene = 1.58×10^4 (E_1) = 5.33×10^{15} (E_2) = 1.27×10^{15} (E_3)
Chang [58]	T = 473–823 K Isothermal n = 1.699–1.865 Average = 1.78	3.501	3.28×10^5
Teng et al. [32]	β = 3–100 K/min	Lump 1 = 125.5 Lump 2 = 178.7 Lump 3 = 243.9	Lump 1 = 2.68×10^{11} Lump 2 = 6.78×10^{13} Lump 3 = 2.86×10^{17}
Kim et al. [15]	β = 2.5–15 K/min Tire sidewall Tire tread	Component 1 = 195.3–210.6 Component 2 = 177.8–212.8 Component 3 = 33.0–48.1 Component 1 = 119.6–136.7 Component 2 = 194.9-229.7 Component 3 = 32.8–46.4	Component 1 = 5.5×10^{13}–6.2×10^{14} Component 2 = 1.3×10^{14}–4.9×10^{16} Component 3 = 1.4×10^2–5.8×10^3 Component 1 = 2.5×10^8–5.7×10^9 Component 2 = 1.1×10^{15}–2.3×10^{18} Component 3 = 1.6×10^2–5.2×10^3
Williams and Besler [12]	β = 5 K/min β = 20 K/min	Tire A = 142.7 Tire B = 102.8 (low) =145.0 (high) Tire C = 130.8 (low) =142.4 (high) Tire A = 90.8 Tire B = 128.3 (low) =137.7 (high) Tire C = 132.7 (low) =134.8 (high)	Tire A = 2.1×10^8 Tire B = 9.3×10^7 (low) =1.1×10^8 (high) Tire C = 1.2×10^8 (low) =2.0×10^8 (high) Tire A = 2.6×10^4 Tire B = 3.3×10^5 (low) =2.1×10^8 (high) Tire C = 1.2×10^8 (low) =4.9×107 (high)
Yang et al. [28]		Oil = 49.1 NR = 207 BR = 215	Oil = 4.01×10^4 NR = 2.36×10^{16} BR = 6.32×10^{14}
Bouvier et al. [11]	T = 645–798 K (372–525 °C) Isothermal	T = 372 K, k = 0.085 min^{-1} T = 675 K, k = 0.183 min^{-1} T = 697 K, k = 0.329 min^{-1} T = 739 K, k = 2.38 min^{-1} T = 775 K, k = 2.80 min^{-1} T = 798 K, k = 7.10 min^{-1}	

Although the authors, Leung and Wang [19], concluded that both models were capable of simulating the three weight-loss regions of the tire pyrolysis process, both models also had some limitations. The three-component simulation model over-predicted the weight loss rate for the second weight loss region (Fig. 5, Leung and Wang [19]). For the three-elastomer model, the values of the activation energies and reaction orders were not estimated from the model, but were based on the works of Yang et al. [16], which were disclosed by the authors. In both model results the simulated masses of the various components were not revealed.

Galvagno et al. [33] also use a three-component model in tire pyrolysis, and the summation of each component's degradation rate gave the overall pyrolysis rate. They matched the degradation of the tire components with the evolution of the volatiles produced using mass spectrometry and FTIR measurements. Galvagno et al. [33] showed that evolution of some products (such as 2-methyl-1,3 butadiene, benzene, toluene, cycloheptadiene, etc.) is representative of the decomposition of the main elastomers mixed into the tire, and calculated the kinetic parameters for the main components.

A similar methodology was used by Lin et al. [17], who modeled styrene–butadiene rubber pyrolysis as three simultaneous, independent reactions. They used the extent of reaction (X), instead of mass fraction in equation (5) such that:

$$\ln\left[\frac{dX}{dt}/\exp\left(-\frac{E_a}{RT}\right)\right] = \ln A + n\ln(1-X). \tag{22}$$

They plotted $\ln\left[\left(\frac{dX}{dt}\right)/\exp-\frac{E_a}{RT}\right]$ versus $\ln(1-X)$ to obtain n, the order of reaction for each reaction. X is similar to the normalized fraction ratio (X) in equation (7). They then plotted the Arrhenius constant ($\ln k$) against the inverse of temperature ($1/T$) to obtain a slope of $-E_a/R$ and an intercept of $\ln A$. Their calculated activation energies and frequency factors for each reaction is given in Table 3. Based on this three-reaction model, they then proposed a reaction scheme where the evolution of volatiles follows the equation:

$$\frac{M_{vi}}{F_i} = 1 - \left[1-(1-n_i)\frac{A_i RT^2}{\beta E_{a,i}}\exp\left(-\frac{E_{a,i}}{RT}\right)\sum_{i=0}^{i}\left[\left(-\frac{RT}{E_{a,i}}\right)\prod_{j=0}^{i}(j+1)\right]\right]\frac{1}{(1-n_i)}, \tag{23}$$

where M_{vi} is the mass fraction of volatiles evolved from F_i, the fraction of the mass of the tire accounting for the ith reaction. This reaction model could be used to predict the volatization of tire attributed to each of the three reactions (i = 1,2,3), and was found to fit well ($R^2 > 0.99$) for various heating rates up to 7 K/min. Lin et al. [34] also employed the same method in the pyrolysis of polybutadiene to obtain the parameters of n, E_a, A and F. However, they observed only two peaks in during the pyrolytic degradation of polybutadiene with increasing temperature, and thus used equations (22) and (23) only for a two reaction model. The R^2 obtained by Lin et al. [34] in this case was 0.981, 0.997 and 0.994 for heating rates of 3, 5 and 7 K/min, respectively.

Similarly, Mui et al. [35] used equation (19) with up to five components and the equations were solved using the Coats–Redfern approximation [64] and the fourth order Runge–Kutta algorithm. The model assumes that the components of the tire are natural rubber (NR), butadiene rubber (BR) and styrene–butadiene rubber (SBR). Their five-component model assumes that BR and SBR both undergo two-step decomposition and NR undergoes only one. The best fit was found with a five-component model using the Runge–Kutta solution at a heating rate of 10 K/min. Due to the limitation of the Coats–Redfern approximation, where kinetic parameters cannot be accurately obtained from multiple mechanisms [65], modeling more components seems to provide a better fitting result than fewer components.

A less arbitrary method of obtaining the number of components/reactions during the pyrolysis of tires was used by Kim et al. [15]. The method involves starting with the highest temperature region, and plotting a straight line on a graph of with $\frac{1}{T}$ against $\ln\left(\frac{1}{m}\frac{dm}{dt}\right)$. This method assumes that the rate of loss in the highest temperature region is due to only one compound, and the other compounds that degraded at lower temperatures presents negligible rate loss in this temperature range. The actual mass of the samples were used in the models. Thus, equation (5) was modified to become:

$$\frac{dm}{dt} = Ae^{-E_a/RT}(m)^n. \tag{24}$$

After obtaining the kinetic parameters and calculating the mass of the last degradable component, Kim et al. [15] were able to work backwards by incorporating this mass into the next degradable tire component and elucidating its kinetic parameters and continue this process until all degradable tire components were elucidated. They then developed a temperature-dependent empirical solution for the pyrolysis time for each component as:

$$\tau_i = \frac{-\ln(1-X_i)}{k_i}, \tag{25}$$

where τ_i is the time taken to pyrolyze component i to an extent of fraction of X_i, the fractional mass conversion.

González et al. [36] divided the thermogravimetric data into three different regions in their kinetic study of tire pyrolysis. They obtained the kinetic parameters using equation (8) while assuming a first-order reaction (n = 1). No R^2 values were given for the model fits to dynamic experimental data, but it was reported the correlation coefficients in all cases were greater than 0.97. Islam et al. [37] also used the three-region approach in their study of the pyrolysis of bicycle, motorcycle and truck tires using equation (8). They obtained an average value of 1.43×10^9 min^{-1} and 103.02 kJ/mol for A and E_a, respectively.

Lopez et al. [38] also used a similar methodology for vacuum pyrolysis of tires. They also assumed a three-step model and used the summation of the three reaction rates as the overall reaction rate as observed on the DTG. They found that the effect of vacuum on the pyrolysis process was significant. The values of activation energy for the pyrolysis of individual components were lower for pyrolysis under vacuum with a reduction of 12 K in the reaction starting temperature, leading to easier devolatilization. The kinetic constant at 503 K for devolatilization of volatile additives at 0.25 atm was 1.7 times higher than that at 1 atm, and that corresponding to styrene–butadiene rubber at 723 K was 2.8 times higher.

Murillo et al. [39,40] did not use the conventional reaction rate model (equation (1)), but fitted their data on CO_2 activation of tire char to four different kinetic models: volume reaction model, modified-volume reaction model, changing grain size model, and random pore model. The volume reaction model is very similar to equation (5) which assumes uniform gas diffusion and homogenous reaction between the gas and the tire particle, with n = 1. The modified-volume reaction model uses a variable rate constant and is expressed as:

$$\frac{d\alpha}{dt} = k_{MV}X(1-X) \tag{26}$$

$$k_{MV}(X) = \chi^{1/\alpha}\alpha[-\ln(1-X)]^{(\alpha-1/\alpha)}, \tag{27}$$

where χ and α are constants to be determined from the conversion data by the least-squares method.

The changing grain size model assumes spherical-shaped particles and follows the unreacted core model under kinetic control:

$$\frac{dX}{dt} = \left(\frac{3}{\tau}\right)\frac{(1-X)^2}{3} \tag{28}$$

$$\tau = \frac{r_g}{b\nu_B k_{CGSM} C^n} \tag{29}$$

$$r_g = \frac{3}{S_{BET}\rho_t} \tag{30}$$

where r_g is the initial grain radius, calculated from the solid surface area.

The changing grain size model allows for arbitrary pore size distributions in the reacting solid, overlapping of pores' surfaces during reaction, and changing surface areas, through a structural characteristic parameter ψ, which in turn is dependent on porosity, ε_0, surface area, S_0, and pore length L_o.

$$\frac{d\alpha}{dt} = \frac{k_{RPM} S_0 C^n}{(1-\varepsilon_0)\rho_M}(1-X)\sqrt{1-\psi\ln(1-X)} \tag{31}$$

$$\varphi = \frac{4\pi L_0(1-\varepsilon_0)}{S_{0_t}^2}, \tag{32}$$

where k_{RPM} is the intrinsic constant rate, C the gasifying agent, p_M the molar density of the reacting solid, n the order of reaction and X the fractional conversion. They calculated the kinetic parameters using these four models and found that the activation energies were very close for all four cases.

In a later work, Aranda et al. [41] also used the random pore model for modeling steam activation of tire char. After obtaining the model parameters, they could predict the maximum reaction rate using the model. Lee and Kim [42] studied the kinetics of tire char gasification in CO_2 after the tires were pyrolyzed. They also used the modified-volume reaction rate model to predict their conversion rate and kinetic parameters, and found that particle size do not influence gasification rate of tire chars below particle sizes of 0.65 mm. Lee and Kim [42] also found that the order of reaction to be 0.68 when CO_2 partial pressures were 0.3–1.0 atm at 950 °C.

Conesa and Marcilla [43] used a modified form of the Arrhenius rate constant in calculating the kinetic parameters. They define a reaction constant for each decomposable fraction in various tire samples as:

$$k_i' = \frac{k_i}{(1-w_{i\alpha})^{n_i-1}}, \tag{33}$$

where k_i is the conventional Arrhenius constant, $w_{i\alpha}$ the weight of fraction i at infinite time and n_i the order of reaction of fraction i. Under this definition of the rate constant, the rate of mass loss for each fraction was then defined as:

$$\frac{dw_i}{dt} = k_i'(w_i - w_{i\alpha})^{n_i}. \tag{34}$$

Together with equation (2), the researchers calculated the various parameters of A, E_a and n of the seven different tire samples by integrating the differential equations using the fourth order Runge–Kutta method. Later, Conesa et al. [44] used similar algorithms on the thermogravimetric data of a Dunlop SP tire, pyrolyzed at three heating rates. They optimized the parameters using the Simplex Flexible method with one, two and three fractions, and found that the model fits best with a three fraction decomposition model.

Conesa et al. [20] also modified this method for modeling the combustion of rubber tires. They included the partial pressure of oxygen for the breakdown of the carbonaceous fraction such that:

$$\frac{\rho dw_i}{dt} = k_0' e^{(-E_{ai}/RT)} w_i^{n_i} p_{O_2}^{n_g}, \tag{35}$$

where p_{O_2} is the partial pressure of oxygen and n_g is the oxygen reaction order. They showed, through the model, that the combustion of tires includes a first step of pyrolysis, and the rate of tire decomposition depended on oxygen partial pressure.

In addition to char reactivity with temperature and oxygen concentration, Larsan et al. [45] modeled tire char combustion to also include particle surface area. The available particle surface area was modeled using a power law model such that:

$$\frac{dX}{dt} = \eta A e^{(-E_{ai}/RT)} \gamma_{O_2}^n (1-X)^{n_m}, \tag{36}$$

where η is an effectiveness factor (from 0 to 1), γ_{O_2} is mole fraction of oxygen, n_m is the power law model parameter, with all other symbols having their usual meaning. They used an iterative, nonlinear least squares method to obtain a set of kinetic parameters at every temperature. Larsan et al. [45] found effectiveness factors ranging from 0.37 to 0.76 at temperatures of 1023–1123 K, indicating mass transfer resistances during steam activation of tire char.

Piatkowski and Steinfeld [46] used a variation of the multicomponent, where they modeled the pyrolysis of tires and steam gasification with the degradation of three components over two stages. They expressed the Arrhenius constant as a function of time, such that:

$$k_i' = k_{o,i} e^{(-E_{ai}/RT(t))} \tag{37}$$

$$T(t) = T_o + \beta t \tag{38}$$

where the heating rate, β is used to provide the temperature, and hence, the Arrhenius reaction rate k_i', and time t, with all other notations having their usual meanings. They then calculate the conversion at time t by considering two different stages, at constant heating and during the isothermal phase.

$$X_i = \left(1 - \exp\left[-\frac{k_{o,i}}{\beta}\int_{T_o}^{T_{iso}} \exp\left(-\frac{E_{ai}}{RT(t_h)}\right)\right] dT\right) + \left(1 - \exp\left[-k_{o,i} t_{iso} \exp\left(-\frac{E_{ai}}{R(T_{iso})}\right)\right]\right), \tag{39}$$

where t_{iso} is the time during the isothermal phase in which conversion of the tire is still occurring. Piatkowski and Steinfeld [46] found that the pyrolysis up to 800 K was well modeled using two components, while the third component was modeled during gasification. A complete conversion also took place only in the isothermal regime of 1476 K.

Babenko et al. [47] proposed a model for the pyrolysis of tires in overheated steam consisting of non-stationary, two-dimensional system of equations of interpenetrating continua. These equations included mass, momentum and energy balances, and reaction kinetics using Arrhenius equations. However, they assumed porosity to be constant, while having a moving porous body front. They concluded that the model showed a good qualitative agreement with experimental data.

Murena et al. [49] created a reaction network, which subdivided the hydrogenative pyrolysis reactions of tires based on the reaction products. They used equation (2) to model various hydrogenative pyrolysis reactions, including the production of heavy liquids, saturated and unsaturated gases and naphthalene. They modeled the results at three temperatures, 618 K, 666 K and 703 K, with 13 rate constants calculated from their model at each temperature.

Suuberg and Aarna [50] used a similar rate expression to equation (33) for the oxidation of pyrolytic tire char, from 670 to 825 K, at oxygen partial pressures from 2 to 19.8 kPa. They found that the order of reaction with respect to oxygen partial pressure varied with burnoff, and was in the range 0.72–0.86. The activation energy of reaction ranged with burnoff from 138 to 150 kJ/mol. The reaction rate did not correlate well with BET surface area, but

did correlate well with the surface area in pores ranging in size from 1.2 to roughly 7 nm in width. They found that a good fit of the pre-exponential factor with surface area was:

$$A = 2.73(\pm 0.7) \times 105 \times SA, \quad (40)$$

where SA (m^2/g) is the DFT surface area and was observed to vary from less than 40 m^2/g at no burnoff to more than 130 m^2/g at 70% burnoff.

Sharma et al. [51] also modeled several simultaneous reactions in the hydrogenative co-pyrolysis of coal and rubber tires. A total of seven reactions were modeled using mass-balanced rate equations developed from equation (2). Consequently, seven rate constants were calculated from the parametrize correlation of the Arrhenius equation (equation (2)):

$$k = k(M)e^{\left(\frac{E_a}{R}\cdot\left\{\frac{1}{T(M)}-\frac{1}{T}\right\}\right)}, \quad (41)$$

where $k(M)$ is the value of k at $T(M)$, which was taken as 673 K. Seven different $k(M)$ (pre-exponential factor, A) and the activation energies and their 95% confidence limits were calculated.

Al-Salem [53] later considered a similar scheme, which also considered the four products of gas, aromatics, liquids and char. These products react through four primary and two secondary side reactions. They found an overall rate constant of $8 \times 10^{-3}\ s^{-1}$ and the overall conversion of tires to products correlated well to the power law.

Grieco et al. [54] constructed a scheme of five partial differential equations to describe the rubber, char and inert reactions, and heat and mass transfer for a tire particle at different radial positions. Heating rates were varied between 0.1 and 1 K/s. The model predictions for temperature profiles and mass loss at different positions within the tire showed that the pyrolysis proceed as a thin front inside the sample. This was explained as the combined effect of the endothermic reaction and heat transport resistance.

Mazloom et al. [55] used experimental data from literature for thermal and catalytic pyrolysis of scrap tires to evaluate two types of lumping models; discrete and continuous lumping model. The lumps were described in terms of the boiling point distribution of the reactant mixture. In the discrete model, the conversion of heavier to lighter lumps was described in terms of series and parallel first order reactions. In the continuous model, the normalized boiling point was used to describe the reactant mixture as a continuous mixture. They implemented an optimization procedure to estimate the model parameters from literature values. Model predictions indicated that although the discrete model could reasonably predict the yields of different products, predictions of the continuous model were very good, especially in thermal pyrolysis.

Miranda at al. [56] used response surface methodology (RSM) in the pyrolysis of mixtures of plastic and rubber tires to prioritize and optimize parameters for liquid yield. Temperature was found to be the most important factor, followed by reaction time. The optimized conditions were found to be 643 K, initial pressure of 0.48 MPa and reaction time of 15 min. However, the researchers conceded that these values are specific to the type of reactor used. A linear model was also found with good fit to the experimental data. Three sets of experimental data were compared with the model results for validation and an experimental deviation of 0.95% was found.

A model to describe the depolymerization for tire specifically with respect to sulfur was proposed by Murena [57]. This work modeled the reactions of sulfur compounds on the basis of a two-step reaction mechanism. In the proposed mechanism, the first step was the dissolution of tire particles into large aggregates; the second step was a slow depolymerization through a cyclic mechanism with the formation of radicals. Kinetic constants of sulfur compound reactions were evaluated by modeling all sulfur compounds as a single group. Their model results were compared with experiments, which were measured using GC-FPD and GC-TCD of gases withdrawn at the end of each run. Only about 1% of sulfur present in the loaded tire was detected in the liquid phase, the remaining being released as H_2S in the gas phase. Their proposed model was:

$$C_s = C_s^o \exp(-k_s t) + C_{VHLS}^o \frac{k_L}{k_S - k_L}(\exp[-k_L T] - \exp[-k_S t]). \quad (42)$$

A few tire pyrolysis works were not done under a slow and constant heating rate (β), but under a constant high temperature. One of the earliest isothermal models was proposed by Bouvier et al. [11]. For each temperature, they obtained sigmoidal curves that were modeled in the parts. Before the point of inflection (i.e. before the conversion reached a steady state), the amount of tire converted to gas or liquid due to pyrolysis was described as:

$$X = 1 - \exp(-k_{(T)} t). \quad (43)$$

After the inflection point, the pyrolysis of tire was described as:

$$X = 1 - (1 - X_i)\exp[-k(t - t_i)]. \quad (44)$$

The extent of reaction or fraction of solid tire remaining, X, after pyrolysis was defined previously (equation (4)).

The rate constant, k was calculated from the above model for each temperature, and an Arrhenius-type equation was fitted:

$$k = \exp\left(20.8 - \frac{15100}{T}\right). \quad (45)$$

The rate constant values for each temperature are given in Table 3.

Bouvier et al. [11] found that model results were in good agreement with experimental points only for temperatures above 739 K. They attributed this good agreement to negligible pyrolysis reaction at lower temperatures and concluded that as temperature decreases, pyrolysis reactions slows down while the extender oil volatizes with a different kinetics that is related to diffusion mechanism.

Chang [58] conducted isothermal pyrolysis from 473 to 823 K, but did not assume a first-order rate in the model. Instead, Chang used equation (22) to obtain the value of n, and then used equation (23) to obtain the kinetic parameters. Chang found a small range of reaction orders from 1.699 to 1.865, and a reaction rate constant (k) that were generally higher than Bouvier's [11]. These values are shown in Table 3.

3.5. Reactor models

In addition to the general kinetic model, there are a few pyrolysis models specific to particular reactor design. Olazar et al. [24] used the integrated form of equation (5) and $n = 1$ to study the kinetics of tire pyrolysis in a conical spouted bed reactor (CSBR). This bench-scale reactor uses a principle similar to a fluidized bed to suspend tire particles in a stream of nitrogen during pyrolysis. They found that the apparent activation energy for the size range between 0.8 and 4.0 mm is significantly lower (41.3 kJ mol^{-1}) than that corresponding to the 0.1–0.8 mm range (121.3 kJ mol^{-1}). These values were also lower than those obtained from DTG and microreactors. The authors attribute this to better heat and mass transfer in the CSBR than the other methods.

The same group of researchers later proposed a scheme that included intermediate and parallel reactions in the formation of products during the pyrolysis of tires [52]. The authors considered five final products: gas, liquids, aromatics, char and their intermediates (Fig. 1). The proposed scheme consisted of four primary reactions in parallel, whose reactant was the original tire, and another three secondary reactions (also in parallel) whose reactant was the intermediate. Using an error-minimization function, they

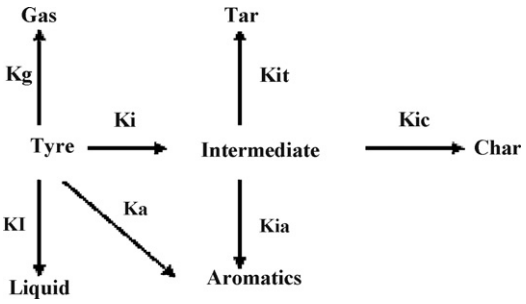

Fig. 1. Scheme of kinetic reactions in CSBR [52].

obtained seven sets of kinetic parameters for the seven equations. Their calculated parameters showed the highest value of activation energies for the formation of aromatics (89.3 kJ/mol) and lowest for the formation of tar from intermediates (14.12 kJ/mol).

Steam gasification of waste tires was studied by Donatelli et al. [48], who used commercial software ChemCAD to model the process in a rotary kiln pilot plant. The numerical model determines the gas composition at equilibrium by following two subsequent operating steps: waste tyres pyrolysis at atmospheric pressure and 400 °C, under inert atmosphere conditions and pyrolysis gas steam gasification at atmospheric pressure and 850 °C. They studied the effect of feeding rate of tires on the resultant gas composition and energy content. However, they observed that there were differences between the model and experimental results. Donatelli et al. [48] attributed this discrepancy between model predictions and experimental data to the assumption of thermodynamic equilibrium in the model, while the experiments were dynamic. They gave the example of char being present in the output of the reactor, which may react with gas mixture components as well as remaining char, leading to a series of secondary reactions not yet considered in modeling reaction. Donatelli et al. [48] concluded that the model cannot yet replace experimentation due to approximations present in the model.

Kalitko et al. [59] developed a model to test the effectiveness of a screw reactor with coil steam superheater for the steam pyrolysis of tires. The modeling work examined the process of fuel consumption, steam generation and waste slime processing. According to this model, 13 min were required to pyrolyze 1000 kg per hour of shredded tires in steam at temperatures 623–723 K. The resulting fuel product included 25–30% of moisture of the partial condensation of steam on the cold surface of tubes, which required subsequent separation of the fuel from this moisture.

Aylón et al. [60] recently developed a model for the pyrolysis of waste tire in a moving bed reactor. The model comprised four sub-models: a hydrodynamic flow sub-model to predict the solid flow pattern inside the reactor, a heat transfer sub-model to predict the temperature profile inside the particle and the energy flux from the surroundings to the tire particle, and a kinetic sub-model to predict solid conversion from reaction time and temperature. The reactor sub-model, shown as equations (46) and (47), integrated all the process variables obtained from the other sub-models, included reactor variables such as length, diameter, characteristic screw dimensions, screw speed, reaction temperature, etc., and made predictions on the pyrolysis of waste tires for a plug-flow reactor.

$$\frac{dX}{dt} = \frac{LS}{t_m m_o} p(X) f(X), \tag{46}$$

where L is the reactor length expressed in meters, S is the reactor section (m^2), t_m is the solid residence time inside the reactor, t is the reaction time, $p(X)$ is the solid density that depends on the conversion and $f(X)$ is the reaction rate, the sum of the decomposition rates for each one of the tire components according to:

$$f(X) = \sum_{i=1}^{N} \left(c_i \frac{dX_i}{dt} \right), \tag{47}$$

where X_i is the solid fractional conversion for sample component i and c_i is a coefficient that expresses the contribution of each single reaction to the mass total loss. A good agreement was found between the conversions of tire particles in the reactor calculated using this model and experimental results.

4. Conclusions

A comprehensive review of the mathematical modeling of tire pyrolysis, conducted by various researchers over the last three decades, was provided. Many models have been proposed for tire pyrolysis, with the majority of them being based on Arrhenius rate equation for reaction kinetics. Most of these models assumed a series of parallel first-order reactions in a multi-component or multi-step model based on the chemical composition of the tires. These models generally produced results that had high correlations with experimental data, and provided a good prediction for tire pyrolysis.

Some of the models reviewed included heat and mass transfer considerations as part of the tire pyrolysis through additional diffusion or conduction equations that directly or indirectly affected the effective temperature of reaction. Geometry and other physical characteristics (e.g. porosity, surface area) considerations were also included in a few models that influence heat and mass transfer dynamically during the pyrolysis process.

Mathematical models were also proposed for the activation and gasification of pyrolyzed tire chars. Most models used the partial pressure or concentration of the activating gas in the Arrhenius equation. Some models also used the physical characteristics of the char such as surface areas in the activation process using similar equations for tire pyrolysis. All models were able to predict the reaction rates and other kinetic parameters of activation or gasification.

Although there were a few attempts at integrating heat, and mass transfer with reaction kinetics, the results have so far not been well correlated with experimental results. There is also a significant knowledge gap between models successfully applied to TGA data and models applied to specific reactors. There is a need for more significant and extensive applications of these models for a wide range of commercial and industrial scale reactors. The development of more universal models for the description of pyrolysis of other carbonaceous materials, such as biomass, hazardous and solid waste, in addition to tires would also be beneficial.

Acknowledgements

One of the authors, Augustine Quek, thanks the World Future Foundation and Beijing Vantone Citylogic Investment Corp. for their joint support of this research.

References

[1] Australian Government, Department of the Environment, Water, Heritage and the Arts (updated: 2010 August 03; cited 2011 January 17). Available from: http://www.environment.gov.au/settlements/waste/tyres/index.html.
[2] P.T. Williams, S. Besler, D.T. Taylor, The pyrolysis of scrap automotive tyres: the influence of temperature and heating rate on product composition, Fuel 69 (1990) 1474–1482.
[3] C. Berrueco, E. Esperanza, F.J. Mastral, J. Ceamanos, P. García-Bacaicoa, Pyrolysis of waste tyres in an atmospheric static-bed batch reactor: analysis of the gases obtained, J. Anal. Appl. Pyrolysis 74 (2005) 245–253.

[4] Rubber Manufacturers Association (RMA), Scrap Tire Markets in the United States 9th Biennial Report, May 2009.
[5] M. Beecham, Global market review of automotive tyres—forecasts to 2014, Aroq Limited UK, 31 July 2008, Pub ID: JA1867566.
[6] United States Environmental Protection Agency (US EPA), Scrap Tires, Basic Information (updated: 2010 September 17, cited 2011 Jan 17). Available from: http://www.epa.gov/osw/conserve/materials/tires/basic.htm.
[7] California Integrated waste management Board (CIWMB), Effects of Waste Tires, Waste Tire Facilities, and Waste Tire Projects on the Environment, April 1996, CIWMB Publication number: 432-96-029.
[8] E.L.K. Mui, D.C.K. Ko, G. McKay, Production of active carbons from waste tyres––a review, Carbon 42 (14) (2004) 2789–2805.
[9] C.K.K. Ko, L.K.E. Mui, S.T.K. Lau, G. McKay, Production of activated carbons from waste tire—process design and economical analysis, Waste Manage. 24 (9) (2004) 875–888.
[10] R. Aguado, M. Olazar, D. Vélez, M. Arabiourrutia, J. Bilbao, Kinetics of scrap tyre pyrolysis under fast heating conditions, J. Anal. Appl. Pyrolysis 73 (2005) 290–298.
[11] J.M. Bouvier, F. Charbel, M. Gelus, Gas–solid pyrolysis of tire wastes—kinetics and material balances of batch pyrolysis of used tires, Resour. Conserv. 15 (3) (1987) 205–214.
[12] P.T. Williams, S. Besler, Pyrolysis-thermogravimetric analysis of tyres and tyre components, Fuel 74 (9) (1995) 1277–1283.
[13] S. Seidelt, M. Müller-Hagedorn, H. Bockhorn, Description of tire pyrolysis by thermal degradation behaviour of main components, J. Anal. Appl. Pyrolysis 75 (1) (2006) 11–18.
[14] O. Senneca, P. Salatino, R. Chirone, A fast heating-rate thermogravimetric study of the pyrolysis of scrap tyres, Fuel 78 (13) (1999) 1575–1581.
[15] S. Kim, J.K. Park, H.-D. Chun, Pyrolysis kinetics of scrap tire rubbers. I. Using DTG and TGA, J. Environ. Eng. 121 (7) (1995) 507–514.
[16] J. Yang, S. Kaliaguine, C. Roy, Improved quantitative determination of elastomers in tire rubber by kinetic simulation of DTG curves, Rubber Chem. Technol. 66 (2) (1993) 213–229.
[17] J.-P. Lin, C.-Y. Chang, C.-H. Wu, Pyrolytic treatment of rubber waste: pyrolysis kinetics of styrene–butadiene rubber, J. Chem. Tech. Biotechnol. 66 (1) (1996) 7–14.
[18] D.Y.C. Leung, C.L. Wang, Kinetic study of scrap tyre pyrolysis and combustion, J. Anal. Appl. Pyrolysis 45 (2) (1998) 153–169.
[19] D.Y.C. Leung, C.L. Wang, Kinetic modeling of scrap tire pyrolysis, Energy Fuels 13 (2) (1999) 421–427.
[20] J.A. Conesa, R. Font, A. Fullana, J.A. Caballero, Kinetic model for the combustion of tyre wastes, Fuel 77 (13) (1998) 1469–1475.
[21] E. Aylón, M.S. Callén, J.M. López, A.M. Mastral, J.M. Murillo, M.V. Navarro, et al., Assessment of tire devolatilization kinetics, J. Anal. Appl. Pyrolysis 74 (1–2) (2005) 259–264.
[22] J.H. Chen, K.S. Chen, L.Y. Tong, On the pyrolysis kinetics of scrap automotive tires, J. Hazard. Mater. 84 (1) (2001) 43–55.
[23] A. Zabaniotou, J. Lagoudakis, E. Toumanidou, G. Stavropoulos, Energetic utilization of used tires, Energy Sources Part A 24 (9) (2002) 843–854.
[24] M. Olazar, R. Aguado, D. Vélez, M. Arabiourrutia, J. Bilbao, Kinetics of scrap tire pyrolysis in a conical spouted bed reactor, Ind. Eng. Chem. Res. 44 (2005) 3918–3924.
[25] K. Unapumnuk, T.C. Keener, M. Lu, S.-J. Khang, Pyrolysis behavior of tire-derived fuels at different temperatures and heating rates, J. Air Waste Manage. Assoc. 56 (5) (2006) 618–627.
[26] L.G. Sachin, M. Giridhar, Catalytic degradation of polybutadiene, Polym. Degrad. Stab. 86 (3) (2004) 529–533.
[27] J.A. Conesa, A. Marcilla, J.A. Caballero, R. Font, Comments on the validity and utility of the different methods for kinetic analysis of thermogravimetric data, J. Anal. Appl. Pyrolysis 58–59 (2001) 617–633.
[28] J. Yang, P.A. Tanguy, C. Roy, Heat transfer, mass transfer and kinetics study of the vacuum pyrolysis of a large used tire particle, Chem. Eng. Sci. 50 (12) (1995) 1909–1922.
[29] J. Yang, C. Roy, Using DTA to quantitatively determine enthalpy change over a wide temperature range by the mass-difference baseline method, Thermochim. Acta. 333 (2) (1999) 131–140.
[30] M.B. Larsen, L. Schultz, P. Glarborg, L. Skaarup-Jensen, K. Dam-Johansen, F. Frandsen, et al., Devolatilization characteristics of large particles of tyre rubber under combustion conditions, Fuel 85 (10–11) (2006) 1335–1345.
[31] A. Quek, R. Balasubramanian, An algorithm for the kinetics of tire pyrolysis under different heating rates, J. Hazard. Mater. 166 (1) (2009) 126–132.
[32] H. Teng, M.A. Serio, M.A. Wojtowicz, R. Bassilakis, P.R. Solomon, Reprocessing of used tires into activated carbon and other products, Ind. Eng. Chem. Res. 34 (9) (1995) 3102–3111.
[33] S. Galvagno, S. Casu, M. Martino, E. Di Palma, S. Portofino, Thermal and kinetic study of tyre waste pyrolysis via TG-FTIR-MS analysis, J. Therm. Anal. Calorim. 88 (2) (2007) 507–514.
[34] J.P. Lin, C.-Y. Chang, C.-H. Wu, S.-M. Shih, Thermal degradation kinetics of polybutadiene rubber, Polym. Degrad. Stab. 53 (3) (1996) 295–300.
[35] E.L.K. Mui, V.K.C. Lee, W.H. Cheung, G. McKay, Kinetic modeling of waste tire carbonization, Energy Fuels 22 (3) (2008) 1650–1657.
[36] J.F. González, J.M. Encinar, J.L. Canito, J.J. Rodríguez, Pyrolysis of automobile tyre waste. Influence of operating variables and kinetics study, J. Anal. Appl. Pyrolysis 58–59 (1) (2001) 667–683.
[37] M.R. Islam, H. Haniu, J. Fardoushi, Pyrolysis kinetics behavior of solid tire wastes available in Bangladesh, Waste Manage. 29 (2) (2009) 668–677.
[38] G. Lopez, R. Aguado, M. Olazar, M. Arabiourrutia, J. Bilbao, Kinetics of scrap tyre pyrolysis under vacuum conditions, Waste Manage. 29 (10) (2009) 2649–2655.
[39] R. Murillo, M.V. Navarro, J.M. López, E. Aylón, M.S. Gallén, T. García, et al., Kinetic model comparison for waste tire char reaction with CO_2, Ind. Eng. Chem. Res. 43 (24) (2004) 7768–7773.
[40] R. Murillo, M.V. Navarro, J.M. López, T. García, M.S. Callén, E. Aylón, et al., Activation of pyrolytic tire char with CO_2: kinetic study, J. Anal. Appl. Pyrolysis 71 (2) (2004) 945–957.
[41] A. Aranda, R. Murillo, T. García, M.S. Callén, A.M. Mastral, Steam activation of tyre pyrolytic carbon black: kinetic study in a thermobalance, Chem. Eng. J. 126 (2–3) (2007) 79–85.
[42] J.S. Lee, S.D. Kim, Gasification kinetics of waste tire-char with CO_2 in a thermobalance reactor, Energy 21 (5) (1996) 343–352.
[43] J.A. Conesa, A. Marcilla, Kinetic study of the thermogravimetric behavior of different rubbers, J. Anal. Appl. Pyrolysis 37 (1) (1996) 95–110.
[44] J.A. Conesa, R. Font, A. Marcilla, Mass spectrometry validation of a kinetic model for the thermal decomposition of tyre wastes, J. Anal. Appl. Pyrolysis 43 (1) (1997) 83–96.
[45] M.B. Larsen, M.L. Hansen, P. Glarborg, L. Skaarup-Jensen, K. Dam-Johansen, F. Frandsen, Kinetics of tyre char oxidation under combustion conditions, Fuel 86 (15) (2007) 2343–2350.
[46] N. Piatkowski, A. Steinfeld, Reaction kinetics of the combined pyrolysis and steam-gasification of carbonaceous waste materials, Fuel 89 (5) (2010) 1133–1140.
[47] V.A. Babenko, V.A. Zhdanok, G.I. Zhuravskii, N.V. Pavlyukevich, Mathematical model of the thermodestruction of worn tires in overheated steam, J. Eng. Phys. Thermophys. 82 (1) (2009) 114–124.
[48] A. Donatelli, P. Iovane, A. Molino, High energy syngas production by waste tyres steam gasification in a rotary kiln pilot plant. Experimental and numerical investigations, Fuel 89 (10) (2010) 2721–2728.
[49] F. Murena, E. Garufi, F. Gioia, Hydrogenative pyrolysis of waste tyres: kinetic analysis, J. Hazard. Mater. 50 (2–3) (1996) 143–156.
[50] E.M. Suuberg, I. Aarna, Kinetics of tire derived fuel (TDF) char oxidation and accompanying changes in surface area, Fuel 88 (1) (2009) 179–186.
[51] R.K. Sharma, J. Yang, J.W. Zondlo, D.B. Dadyburjor, Effect of process conditions on co-liquefaction kinetics of waste tire and coal, Catal. Today 40 (4) (1998) 307–320.
[52] M. Olazar, G. Lopez, M. Arabiourrutia, G. Elordi, R. Aguado, J. Bilbao, Kinetic modelling of tyre pyrolysis in a conical spouted bed reactor, J. Anal. Appl. Pyrolysis 81 (1) (2008) 127–132.
[53] S.M. Al-Salem, P. Lettieri, J. Baeyens, Kinetics and product distribution of end of life tyres (ELTs) pyrolysis: a novel approach in polyisoprene and SBR thermal cracking, J. Hazard. Mater. 172 (2–3) (2009) 1690–1694.
[54] E. Grieco, M. Bernardi, G. Baldi, Styrene–butadiene rubber pyrolysis: products, kinetics, modeling, J. Anal. Appl. Pyrolysis 82 (2) (2008) 304–311.
[55] G. Mazloom, F. Farhadi, F. Khorasheh, Kinetic modeling of pyrolysis of scrap tires, J. Anal. Appl. Pyrolysis 84 (2) (2009) 157–164.
[56] M. Miranda, F. Pinto, C.I. GulyurtluI, N.A. Nogueira, A. Matos, Response surface methodology optimization applied to rubber tyre and plastic wastes thermal conversion, Fuel 89 (9) (2010) 2217–2229.
[57] F. Murena, Kinetics of sulphur compounds in waste tyres pyrolysis, J. Anal. Appl. Pyrolysis 56 (2) (2000) 195–205.
[58] Y.-M. Chang, On pyrolysis of waste tire: degradation rate and product yields, Resour. Conserv. Recycl. 17 (2) (1996) 125–139.
[59] V.A. Kalitko, M.Y.W. Chun, V.A. Zhdanok, B.T.Y. Ching, Steam thermolysis of discarded tires: testing and analysis of the specific fuel consumption with tail gas burning, steam generation, and secondary waste slime processing, J. Eng. Phys. Thermophys. 82 (2) (2009) 236–245.
[60] E. Aylón, A. Fernández-Colino, R. Murillo, G. Grasa, M.V. Navarro, T. García, et al., Waste tyre pyrolysis: modelling of a moving bed reactor, Waste Manage. 30 (12) (2010) 2530–2536.
[61] E.L.K. Mui, W.H. Cheung, K.C.V. Lee, G. McKay, Compensation effect during the pyrolysis of tyres and bamboo, Waste Manage. 30 (5) (2010) 821–830.
[62] J. Yang, P.A. Tanguy, C. Roy, Numerical model for the vacuum pyrolysis of scrap tires in batch reactors, AIChE J. 41 (6) (1995) 1500–1512.
[63] Z. Korenova, M. Juma, J. Annus, J. Markos, L. Jelemenesky, Kinetics of pyrolysis and properties of carbon black from a scrap tire, Chem. Pap.—Chem. Zvesti 60 (6) (2006) 422–426.
[64] W. Coats, J.P. Redfern, Kinetic parameters from thermogravimetric data, Nature 201 (1964) 68–69.
[65] R. Ebrahimi-Kahrizsangi, M.H. Abbasi, Evaluation of reliability of Coats–Redfern method for kinetic analysis of non-isothermal TGA, Trans. Nonferrous Met. Soc. China 18 (1) (2008) 217–221.
[66] H.E. Kissinger, Reaction kinetics in differential thermal analysis, Anal. Chem. 29 (11) (1957) 1702–1706.